International Journal of Emerging Science and Engineering (IJESE)
ISSN: 2319–6378 (Online), Volume-12 Issue-7, June 2024

Predictive Controller Strategies for Electrical Drives System using Inverter System

Suraj R. Karpe, S. A. Deokar, U. B. Shinde

Abstract: Advanced control strategies in power electronics include Predictive controller of current (P CURRENT CONTROL) and Predictive controller of torque (P TORQUE CONTROL). To operate a SRM or an induction machine, the Predictive controller of torque (P TORQUE CONTROL) approach analyses the stator flux and electromagnetic torque in the cost function (IM), and the Predictive controller of current (P CURRENT CONTROL) method [1,2] takes errors between the current reference and the measured current into account in the cost function. The switching vector selected for usage in IGBTs reduces the error between the references and the predicted values. The system restrictions are easy to include [4, 5]. The weighting component is not required. Together with the P TORQUE CONTROL and P CURRENT CONTROL systems, the SRM method is the most practicable direct control technique since it doesn't require a modulator and offers 10% to 30% more power than an induction motor [3]. With the same current, an induction motor can only generate between 70% and 90% of the force generated by an SRM due to its lagging power factor. SRM approach decreases 23% more THD in torque, speed, and stator current when P CURRENT CONTROL and P TORQUE CONTROL methods with a 15-level H-bridge multilevel inverter are compared to P CURRENT CONTROL and P TORQUE CONTROL methods with a 15-level H-bridge multilevel inverter utilising an induction motor [21]. The transistors are only swapped when necessary to maintain the limits of torque and flux, which minimises switching losses. To improve the efficiency of a multilevel inverter, semiconductor switches are switched in a specific pattern. In contrast to the P TORQUE CONTROL and P CURRENT CONTROL approaches using a 2-level voltage source inverter, the 15-level H-bridge multilevel inverter employed in this study, coupled with SRM and IM, gives outstanding torque and flux responses and achieves robust and stable operation. This unique strategy quickly caught the interest of academics due to its simple algorithm and high performance in both steady and transient modes [8].

Keywords: Voltage Source Inverter, Predictive Controller of current (P CURRENT CONTROL), Predictive Controller of Torque (P TORQUE CONTROL), Synchronous Reluctance Motor (SRM), Electrical Motors, 15-level H-Bridge Inverter

Manuscript received on 05 April 2024 | Revised Manuscript received on 11 June 2024 | Manuscript Accepted on 15 June 2024 | Manuscript published on 30 June 2024.

**Correspondence Author(s)*

Dr. Suraj R. Karpe*, Associate Professor, Department of Electrical Engineering, CSMSS Chh. Shahu College of Engineering, Aurangabad (Maharashtra), India. E-mail: surajkarpe007@gmail.com, ORCID ID: 0000-0002-2812-8757

Sanjay Deokar, Department of Electrical Engineering, CSMSS Chh. Shahu College of Engineering, Aurangabad (Maharashtra), India. E-mail: s_deokar2@rediffmail.com, ORCID ID: 0000-0003-0603-9136

Dr. Ulhas B. Shinde, Principal, CSMSS Chh. Shahu College of Engineering, Aurangabad (Maharashtra), India. E-mail: drshindeulhas@gmail.com, ORCID ID: 0009-0005-2424-9841

I. INTRODUCTION

Predictive controller of current (P CURRENT CONTROL) and Predictive controller of torque are promising methods (P TORQUE CONTROL). The FCS-P TORQUE CONTROL technique shows several advantages in addition to reducing torque ripples, such as its ease, straightforwardness, simple implementation, and quick dynamic responses of the algorithm. Calculating the necessary control signals in preparation is the fundamental tenet of the model predictive direct torque control (MPDTC) method [6].

The MPDTC Method does not require pulse width modulation. The control technique requires the inverter type. During MPDTC, the P TORQUE CONTROL and P CURRENT CONTROL method computes all possible voltage vectors, and then selects the best one using an optimum cost function [7]. According to the papers [8] [9], the P CURRENT CONTROL and P TORQUE CONTROL techniques have been extensively studied and

Applied in numerous operational contexts to date. Model Predictive Control (MPC) has garnered considerable attention and demand in the power electronics systems and industrial machines community in recent years. The MPC control strategy, which was created for process control applications and first introduced in 1970, is extensively used in the sector and has a variety of reported applications [4]. The central tenet of model predictive control methods is that they base choices not on the system's prior state, but instead on the anticipated behaviour of the state variables and the proper offline or online selection of the controlled variables.MPC is also known as receding horizon control because its primary function is to continuously adjust the prediction horizon, thereby representing an infinite prediction horizon. The present development and fresh focus in the MPC field described in [5]. The MPC is sometimes used to regulate power converters, despite its straightforward design, due to its numerical intricacy, which puts a strain on the processors. Due to the development of new, high-speed processors, MPC utilisation has increased today. In [6], a multilayer inverter and VSI are controlled by an MPC, and the VSI's discrete-time model is used to forecast the load current for all potential inverter-generated voltage vectors. According to this, MPC has been extensively used in many power electronics applications, including matrix converters [8] and the management of different industrial drives like DC-DC converters [7].

Based on a linearized state-space representation that represents the dynamic operation, MPDTC can also be used to regulate the speed of permanent magnet synchronous motors and induction motors [9] [10].

The P TORQUE CONTROL method has two drawbacks when MPC compares it to the DTC method: it relies on speed and requires longer computation times. The P TORQUE CONTROL technique takes longer because the optimal cost function is implemented; however, this issue can be readily fixed with improved and faster microprocessing units [10], [11]. In the prediction phases of the conventional P TORQUE CONTROL method for induction machine (IM) and SRM motor applications, the rotor electrical speed is necessary. The estimated speed as well as the observed speed values affect the projected stator current values.

In modern times, connecting a semiconductor switch directly to a system with medium-sized power networks will cause problems. To address the challenges of middle voltage, high voltage, and exceptionally high voltage energy applications, a multilevel converter system has been developed. A multilevel inverter can use renewable energy as a supply and achieve high power levels. For high-power applications, green energy sources such as solar, fuel cells, and wind can be readily interfaced with a tiered inverter structure. For the past thirty years, the multiple-inverter concept has been in use. The multilevel inverter (MLI) has gained considerable popularity recently and has continued to grow in popularity over time. Because several power semiconductor devices and capacitors were used as voltage sources, MLI was able to produce a stepwise voltage pattern with reduced harmonic distortion. The ability of MLI to minimise the voltage burden on power switches, dv/dt ratio, and standard mode voltage, thereby improving output quality [12,13], is just one of its many advantages. Diode-clamped multilevel inverters, Cascaded Multilevel Inverters, and Flying Capacitor Multilevel Inverters are a few examples of MLI designs. Out of these, the H-Bridge multilevel inverter has several benefits, including the ability to operate at lower switching frequencies, generate output voltages with extremely low distortion, draw input current with very low distortion, and produce smaller common-mode (CM) voltages.

In this research, 2-level voltage source inverters are compared to P TORQUE CONTROL and P CURRENT CONTROL techniques with 15-level H-bridge multilevel inverters using SRM and IM. The modelling method was applied to both investigations. When using SRM instead of an induction motor, the P CURRENT CONTROL and P TORQUE CONTROL technique with a 15-level H-bridge multilevel inverter lowers THD by 23% in terms of torque, speed, and stator current [10] [21]. Switching loses reduction through THD minimization is discussed in this article. The transistors are only swapped when necessary to maintain the limits of torque and flux, which minimises switching losses. This novel method quickly caught the interest of academics due to its straightforward formula and robust findings in both constant and transient states [8,14,15].

II. SRM MODELING

Here, a synchronous machine without a damper winding is employed to develop the mathematical model for vector control of the SRM, along with the dynamics of the field current. The synchronously revolving rotor reference frame is used to translate stator coil numbers into the synchronous rotating reference frame, which rotates at the same speed as the rotor. The SRM without damper winding model, built in the rotor reference frame, exhibits a sinusoidal induced EMF, limited core losses, and no field current dynamics. The rotor flux is assumed to be constant, concentrated along the d-axis, and negative along the q-axis at a specific working location in the creation of indirect vector-controlled induction motor drives. When the location of the rotor magnets is taken into account, it is possible to calculate the immediate induced emf independently of the stator voltages and currents, and subsequently determine the stator currents and torque of the machine. The corresponding q- and d-axis stator windings are converted to the reference frames that revolve at rotor speed when a rotor reference frame is taken into account. The final requirement is that the magnetic fields of the rotor and stator rotate at the same speed and that the windings on the q- and d-axes of the stator are in phase with the rotor magnet axis, which is the d-axis in the design [17,18].

The following describes a complicated equation-based mathematical description of an SRM in the context of a rotor:

Voltage equations are given by:

$$V_d = R_s i_d - \omega_r \lambda_q + \frac{d\lambda_d}{dt} \quad [1]$$

$$V_q = R_s i_q - \omega_r \lambda_d + \frac{d\lambda_q}{dt} \quad [2]$$

Flux linkage is given by

$$\lambda_q = L_q i_q \quad [3],$$

$$\lambda_d = L_d i_d + \lambda_f \quad [4]$$

Substituting Equations 3 and 4 in 1 and 2, we get,

$$V_q = R_s i_q - \omega_r (L_d i_d + \lambda_f) + \frac{d(L_q i_q)}{dt} \quad [5]$$

$$V_d = R_s i_d - \omega_r L_q i_q. + \frac{d}{dt}(L_d i_d + \lambda_f) \quad [6]$$

Arranging equations 5 and 6 in matrix form,

$$\begin{pmatrix} V_q \\ V_d \end{pmatrix} = \begin{pmatrix} R_s + \frac{dL_q}{dt} & \omega_r L_d \\ -\omega_r L_q & R_s + \frac{dL_d}{dt} \end{pmatrix} \begin{pmatrix} i_q \\ i_d \end{pmatrix} + \begin{pmatrix} \omega_r \lambda_f \\ \frac{d\lambda_f}{dt} \end{pmatrix} \quad [7]$$

The developed motor torque is given by

$$T_e = \frac{3}{2}\left(\frac{P}{2}\right)(\lambda_d i_q - \lambda_q i_d) \quad [8]$$

$$T_e = \frac{3}{4} P[\lambda_f i_q + (L_d - L_q) i_q i_d] \quad [9]$$

$$T_e = T_L + B\omega_m + J\frac{d\omega_m}{dt} \quad [10]$$

Solving for rotor mechanical speed from equation 10, we get,

$$\omega_m = \int \left(\frac{T_e - T_L - B\omega_m}{J}\right) dt \quad [11]$$

And the rotor electrical speed is

$$\omega_r = \omega_m \left(\frac{P}{2}\right) \quad [12]$$

III. H-BRIDGE INVERTER

Figure 1 shows an n-level H-bridge cascaded converter in a single-phase arrangement. A single-phase full-bridge/or H-

Published By:
Blue Eyes Intelligence Engineering
and Sciences Publication (BEIESP)

bridge converter is attached to each distinct DC source.

By linking the DC source to the AC output through various configurations of the four switches (S1, S2, S3, and S4), each inverter can produce three distinct output voltage levels: +Vdc, 0, and -Vdc. Switches S1 and S4 are activated for voltage level +Vdc, while S2 and S3 are activated for voltage level -Vdc. Switches S1 and S2, or S3 and S4, can be turned on to achieve zero-level power. To create the multilayer voltage waveform, the AC outputs of all the synthesised full-bridge inverter levels are linked in series and added together. A cascade inverter has n layers of output phase voltage, where n = 2l+1, where l is the number of independent DC sources. Using (n-1)/2 distinct DC sources and (n-1)/2 full bridges, a sample phase voltage waveform for an n-level cascaded H-bridge inverter is shown. The output phase voltage is generalized for use as

$$v = v_{a1} + v_{a2} + v_{a3} + v_{a4} + v_{a5} \dots \dots \dots + v_{an} \quad [13]$$

The matching stepwise waveform's Fourier transform is as follows [9, 5]:

$$V(\omega t) = \frac{4V_{dc}}{\pi}\sum[\cos(n\theta_1) + \cos(n\theta_2) + \cdots + \cos(n\theta_l)]\frac{\sin(n\omega t)}{n} \quad [14]$$

where n = 1,3,5,7.

By deciding on conducting angles, 1, 2,..., l, that minimise total harmonic distortion (THD). These propagation angles primarily remove lower frequency harmonics of the fifth, seventh, eleventh, and thirteenth orders in the output [16,19]. The following succinctly summarises the significant advantages and disadvantages of cascaded H-bridge multilevel inverters: Benefits: • There are more than twice as many potential output voltage values (n = 2l+1) as there are DC sources.

• The H-bridge line enables modular packing and layout. Enable a quicker and more affordable production procedure. Cons: Each H-bridge requires a separate DC source, which can cause fluctuations in DC source power.Units

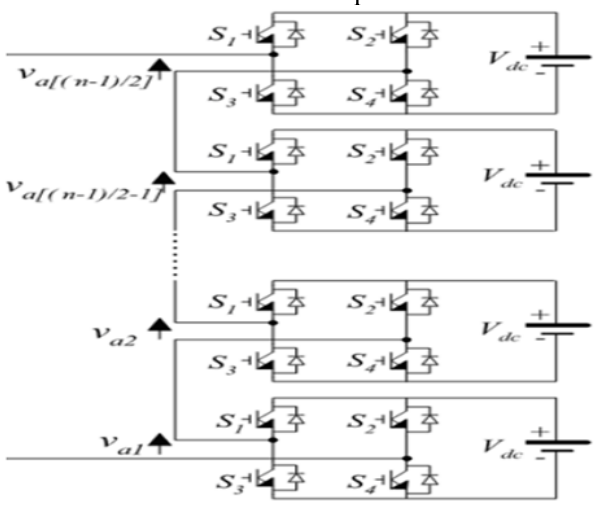

Fig. 1: Leg of Cascaded H-Bridge Multilevel Structure

IV. SWITCHING LOSSES

Transistor losses can be divided into two groups: switching losses (appearing when the devices are switched on or off) and conduction losses. (as a result of ohmic impedance). The commutated current, applied voltage, and semiconductor characteristics all have an impact on these losses. By considering that in a VSI inverter, the voltage seen by each semiconductor is always half the total DC-link voltage, the optimal switch turn-on (energy) loss power can be calculated.

$$E_{on} = e_{on}\frac{1}{2}V_{dc}i_{ph} \quad [15]$$

whereiph is the phase current and aeon is a constant. For the turn-off losses of the perfect switch, an equation with the constant eoff is obtained. Usually, eoff is an order of magnitude larger than aeon. A diode's switch-on losses are virtually nonexistent. The reverse recovery losses, also known as turn-off losses, are erratic in commutated phase current but constant in voltage. Similar to how they affect switching losses, the applied voltage and phase current both impact conduction losses. Despite variations in the neutral point, the DC connection voltage remains consistent. The phase current is the result of adding the fundamental component and the current ripple, and it relies only on the working point—which is determined by the torque and speed—and not on the switching pattern. For a 3-level inverter, the ripple is typically in the range of 10%, which makes it reasonable to assume that conduction losses are independent of the switching pattern.

V. VOLTAGE SOURCE INVERTER

In this study, the P TORQUE CONTROL and P CURRENT CONTROL techniques are also used with a two-level voltage source inverter. Fig. 2 displays the inverter's structure and its practical voltage vectors. The following vector can be used to represent the transitioning state S:

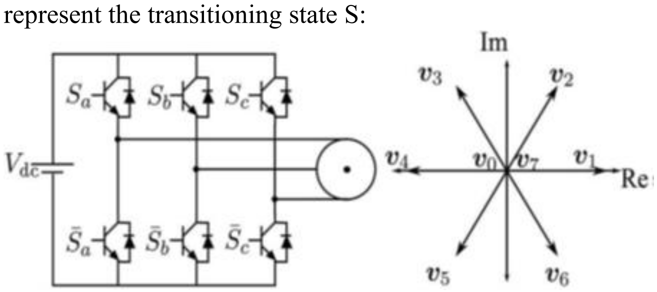

Fig. 2. Left: Two-Level Voltage Source Inverter; Right: Voltage Vectors

The eight voltage vectors represented by the stator voltage space vector can be described as follows by the switching stages and the DC-link voltage, Vdc:

$$V_s(S_a, S_b, S_c) = \left(\frac{2}{3}\right)V_{dc}\left(V_a + V_b e^{j\left(\frac{2}{3}\right)} + V_c e^{j\left(\frac{4}{3}\right)}\right) \quad [16]$$

Where V_{dc} The DC-link voltage is the DC voltage, and the Park's Transformation coefficient of 2/3 is the coefficient. The line-to-line values of the AC motor, which can be written as follows, can be used to obtain the equation:

$$V_{ab} = V_{dc}(S_a - S_b) \quad [17]$$

$$, V_{bc} = V_{dc}(S_b - S_c) \quad [18]$$

$$V_{ca} = V_{dc}(S_c - S_a) \quad [19]$$

The stator phase voltages (line-to-neutral voltages) are required and can be obtained from the line-to-line voltages as follows.

Published By:
Blue Eyes Intelligence Engineering
and Sciences Publication (BEIESP)

$V_a = (V_{ab} - V_{ca})/3$ [20]
$, V_b = (V_{bc} - V_{ab})/3$ [21]
$, V_c = (V_{ca} - V_{bc})/3$ [22]

If the line-to-line voltages in terms of the DC-link voltage, *Vdc*, and switching states are substituted into the stator phase voltages, it gives:

$V_a = \left(\frac{1}{3}\right) V_{dc}(2S_a - S_b - S_c)$ [23]

$V_b = \left(\frac{1}{3}\right) V_{dc}(-S_a + 2S_b - S_c)$ [24]

$V_a = \left(\frac{1}{3}\right) V_{dc}(-S_a - S_b + 2S_c)$ [25]

The equation can be summarized as:

$V_a = Re(V_s) = \left(\frac{1}{3}\right) V_{dc}(2S_a - S_b - S_c)$ [26]

$V_b = Re(V_s) = \left(\frac{1}{3}\right) V_{dc}(-S_a + 2S_b - S_c)$ [27]

$V_c = Re(V_s) = \left(\frac{1}{3}\right) V_{dc}(-S_a - S_b + 2S_c)$ [28]

$S = \frac{2}{3}(S_a + aS_b + a^2 S_c)$ [29]

where $a = e^{j\frac{2\pi}{3}}$, S_i= 1 meansS_iON, $\overline{S_i}$Means OFF, and i = *a, b, c*. The voltage vector, Vis, is related to the switching states by:

$v = V_{dc}S$ [30]

where Vdc is the DC-link voltage

VI. PREDICTIVE DIRECT CONTROL METHODS FOR SRM

A. Predictive Control of Current (P Current Control)

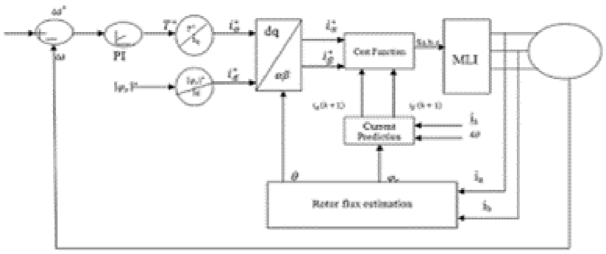

Fig. 3 P Current Control

Predictive Using only the expected stator currents in the set reference frame, current control (P CURRENT CONTROL) is used to regulate the multiphase drive. As shown in Fig. 3, current references are acquired in the rotating reference frame using an exterior PI speed control loop and a constant d-component current. These references are then mapped in the fixed reference frame and used in the cost function. Multiphase drives with various numbers of windings have been used to execute this straightforward predictive controller system [10].

Sinusoidal stator current standards in the a-b-c phase coordinates are necessary to generate the appropriate electric power. The control objective is transformed into either a null or non-null reference stator current vector in the x-y plane, depending on the multiphase machine used. The reference stator current vector in the - plane is constant in amplitude but varies its electrical angle in a circular trajectory. MPC-based predictive current controller with an external speed control loop. The SRM model, stator current is as follows:

$$i_s = -\frac{1}{R_\sigma}\left(\left(L_\sigma.\frac{di_s}{dt} - K_r.\left(\frac{1}{\tau_r} - j.\omega\right).\varphi_r\right) - v_s\right) \quad [31]$$

where$K_r = \frac{L_m}{L_r}$, $R_\sigma = R_s + K_r^2.R_r$ *and* $L_\sigma = \sigma.L_s$

The forward Euler discretization is as

$$\frac{dx}{dt} \cong \frac{x(k+1) - x(k)}{T_s} \quad [32]$$

where Ts is the sampling time of the system.

Using (8) and (9), the stator current can be predicted as

$$\bar{\iota}_s(k+1) = \left(1 - \frac{T_s}{T_\sigma}\right).i_s(k) + \frac{T_s}{T_\sigma}.\frac{1}{R_\sigma}.\left[K_r.\left(\frac{1}{T_r} - j.\omega(k)\right).\varphi_r(k) + v_s(k)\right] \quad [33]$$

$where\ T_\sigma = \sigma.\frac{L_s}{R_\sigma}$

The cost function is represented as below:

$$g_j = \sum_{h=1}^{N}\left\{\left|i_\alpha^* - i_\alpha(k+h)_j\right| + \left|i_\beta^* - i_\beta(k+h)_j\right|\right\} \quad [34]$$

From (11), it follows that the present reference generation is required to finish designing the P CURRENT CONTROL technique. The P CURRENT CONTROL method's block layout is illustrated in Fig. 2. A speed PI controller generates the torque reference, and the reference to rotor flux magnitude is taken to be a fixed number.

The related standard numbers for the torque- and field-producing currentsi_d^* and i_q^* are produced by

$i_d^* = \frac{|\varphi_r|^*}{L_m}$ [35] ,

$i_q^* = \frac{2}{3}\frac{L_r}{L_m}\frac{T^*}{|\varphi_r|^*}$ [36]

In the cost function, the state's current values in the *αβ* frame are required. The inverse Park transformation is presented to satisfy this requirement as follows:

$$\begin{pmatrix}\alpha\\ \beta\end{pmatrix} = \begin{pmatrix}cos(\theta) & -sin(\theta)\\ sin(\theta) & cos(\theta)\end{pmatrix}\begin{pmatrix}d\\ q\end{pmatrix} \quad [37]$$

B. Predictive Control Of Torque (P Torque Control)

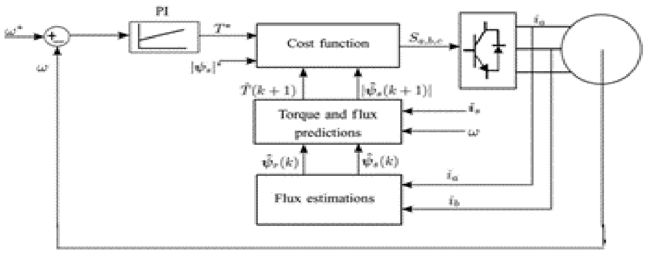

Fig. 4 MPC-based Predictive Controller of Torque with an Outer Speed Control Loop

For three-phase, two-stage induction motor systems, Predictive Controller of Torque (P TORQUE CONTROL) based on FCS-MPC is shown in Fig. 4. The stator flux and torque are controlled variables, and an internal P TORQUE CONTROL and an external PI-based speed control run the process. The torque reference is provided by an external PI based on the speed error, while the stator flux reference is fixed to its usual value for base speed operation. After evaluating the cost function [20] [22], the switching condition with a decreased cost (J) is then utilised with the VSI. To improve P TORQUE CONTROL performance, a changed cost function that aimed to not only control stator flux and produce torque but also set a maximum attainable stator limit was provided in [17].

Retrieval Number: 100.1/ijese.E41140612523
DOI: 10.35940/ijese.E4114.12070624
Journal Website: www.ijese.org

Published By:
Blue Eyes Intelligence Engineering
and Sciences Publication (BEIESP)

Torque and flow forecasts, as well as the creation of a cost function, are at the heart of P TORQUE CONTROL. In the predictive algorithm, the stator flux prediction can be obtained as

$$\bar{\varphi}_s(k+1) = \varphi_s(k) + T_s.v_s(k) - R_s.T_s.i_s(k) \quad [38]$$

The electromagnetic torque can be

$$\bar{T}(k+1) = \frac{3}{2}.p.Im\{\bar{\varphi}_s(k+1)^*.\bar{\imath}_s(k+1)\} \quad [39]$$

The classical cost function for the P TORQUE CONTROL method is

$$g_j = \sum_{h=1}^{N}\{|T^* - \bar{T}(k+1)_j| + \lambda.\|\|\varphi_s^*\| - \|\bar{\varphi}_s(k+h)_j\|\|\} \quad [40]$$

VII. RESULTS

A. P Current Control and P Torque Control Method with SRM and IM using 15-Level Inverter

A 15-level multilayer inverter was used to model P CURRENT CONTROL and P TORQUE CONTROL for a 4-pole induction machine and compare it to a 2-level voltage source inverter. The induction motor has the following specifications: 5 HP, 440V, 50Hz, and 1440 RPM. The following motion parameters will be used for all simulations:

Table. 1: Induction Motor Parameters

Resistance of stator (ohms)	1.403
Resistance of rotor (ohms)	1.395
Self-inductance of stator (H)	= 0.005839
Self-inductance of rotor (H)	0.005839
Rotor Mutual Inductance (H)	0.2037
Number of poles	= 4
Inertia (kg.m^2)	0.0005
Time of Sampling	= 1 Sec

A 15-level multilayer inverter was used to model P CURRENT CONTROL and P TORQUE CONTROL for a 4-pole SM and compare it to a 2-level voltage source inverter. The following motion parameters will be used for all simulations. Table II lists the characteristics of the SRM motor. The following motion parameters will be used for all simulations:

Table. 2: SRM Parameters

Phase resistance Stator Rs	= 4.3
Arm. Inductance	= 0.0001
Linkage established by magnets	= 0.05
Voltage Constant	= 18.138
Torque Constant	= 0.15
Inertia, friction factor, pole pairs	0.000183
Friction factor	= 0.001
Pole pairs	= 2
Initial conditions ia,ib(A)]	= [0,0, 0,0]
Sampling Time	= 1

For the predictive approach, it is necessary to calculate the electromagnetic tension T(k + 1) and the next-step stator flow s(k + 1). The stator flow prediction can be created by discretizing the voltage model (1) with (9) asFigures 5, 6, and 10 compare the modelling findings of the P CURRENT CONTROL method and the P TORQUE CONTROL method with IM using a 15-level inverter to those of the P CURRENT CONTROL method and the P TORQUE CONTROL method with SRM using the same inverter [10]. The images indicate that both techniques behave similarly and effectively at this stage of the procedure. The P CURRENT CONTROL technique has a slightly better current reaction, but the P TORQUE CONTROL method has fewer torque ripples than the P CURRENT CONTROL method does. Results across the whole speed spectrum are investigated in the models. The motor goes from a positive nominal speed to a negative nominal speed. The rotor current, measured speed, and measured force are all monitored throughout this dynamic process. The waves of the two techniques are very similar. The same exterior speed PI factors cause them to have nearly identical settling times to finish this reversal process. When compared to the P CURRENT CONTROL technique, the torque waves produced by the P TORQUE CONTROL method are marginally smaller. Based on these models, we can say that two techniques can behave well at steady states with the complete load and perform well across the entire speed range. THD minimisation was the strategy employed in this research to minimise total harmonic distortion (THD). Total harmonic distortion (THD) has been precisely calculated in this research using MATLAB 2013. The recommended method performs better in terms of Total Harmonic Distortion when compared to conventional methods for speed, torque, and stator current in fleeting situations (THD).Figs. 5(a), (b), and 6(a), (b), respectively, depict the related speed, torque, and stator current reactions of the P TORQUE CONTROL and P CURRENT CONTROL systems using SRM with a 15-level converter (c). In the P CURRENT CONTROL and P TORQUE CONTROL using SRM with a 15-level converter, Figures 9(a),(b),(c) and Figure 10(a),(b),(c) respectively show the THD in speed, electromagnetic torque, and stator current. Figs. 7(a), (b), and 8(a), (b), respectively, show the corresponding speed, torque, and stator current reactions of the P TORQUE CONTROL and P CURRENT CONTROL systems with a 15-level converter using IM (c). The THD in speed, electromagnetic torque, and stator current for the P CURRENT CONTROL and P TORQUE CONTROL techniques with IM using a 15-level converter are shown in Figures 11(a), (b), and 12(a), (b), respectively. According to the article [10], P CURRENT CONTROL and P TORQUE CONTROL decrease THD in speed, torque, and rotor current by roughly 5.3% and 4.8%, respectively, in the conventional system. When compared to the article [10] shown in Table 3, the suggested P CURRENT CONTROL and P TORQUE CONTROL system with 15-level inverter is shown to be better to the standard one by the THD in speed, torque, and stator current with P CURRENT CONTROL and P TORQUE CONTROL being decreased by roughly 23% and 23%, respectively.

B. P Current Control and P Torque Control Method with SRM and IM using 2-Level Inverter

Figures 3 and 4 depict the MATLAB and Simulink models of the P CURRENT CONTROL and P TORQUE CONTROL methods with SRM using a 2-level inverter. The external PI speed regulators are configured with the same settings to facilitate comparison between the two approaches. The simulation results of the P CURRENT CONTROL method and the P TORQUE CONTROL method with SRM using a 2-level inverter are shown in Fig. 13(a),(b),(c) and Fig. 14 (a),(b),(c) compared with the simulation results of the.

Published By:
Blue Eyes Intelligence Engineering
and Sciences Publication (BEIESP)

P CURRENT CONTROL method and the P TORQUE CONTROL method with IM using a 2-level inverter shown in Fig.15 (a),(b),(c), Fig.16 (a),(b),(c) respectively [10]. The images indicate that both techniques behave similarly and effectively at this stage of the procedure. The P CURRENT CONTROL method has a slightly better current response; however, the torque ripples of the P TORQUE CONTROL method are lower than those of the P CURRENT CONTROL method. The performances in the whole speed range are investigated in the simulations. The motor rotates from positive nominal speed to negative nominal speed. During this dynamic process, the measured speed, the torque, and the stator current are observed. Both methods have very similar waveforms. They each have almost the same settling time to complete this reversal process due to the same external speed PI parameters. The torque ripples of the P TORQUE CONTROL method are slightly lower than those of the P CURRENT CONTROL method. From these simulations, we can conclude that both methods can work well across the entire speed range and exhibit good behaviour with full load at steady states.

The method used in this study to minimise switching losses is THD minimization. In this study, total harmonic distortion (THD) has been accurately computed using MATLAB 2013. The recommended method performs better in terms of Total Harmonic Distortion when compared to conventional methods for speed, torque, and stator current in fleeting situations (THD). The corresponding speed, torque, and stator current responses of the P TORQUE CONTROL and P CURRENT CONTROL systems using SRM with a 2-level converter are shown in Figs. 13 (a), (b), (c), and 14 (a), (b), (c), respectively. Figures 17(a),(b),(c) and Figure 18(a),(b),(c) respectively demonstrate the THD in speed, electromagnetic torque, and stator current in the P CURRENT CONTROL and P TORQUE CONTROL using SRM with a 2-level converter. The related speed, torque, and stator current responses of the P TORQUE CONTROL and P CURRENT CONTROL systems using IM with a 2-level inverter are similarly depicted in Fig. 15(a), (b), (c), and Fig. 16(a), (b), (c). The THD in speed, electromagnetic torque, and stator current for a 2-level converter using the P CURRENT CONTROL and P TORQUE CONTROL methods are depicted in Figs. 19(a), (b), and 20(a), (b), respectively. According to the article [10], P CURRENT CONTROL and P TORQUE CONTROL decrease THD in speed, torque, and rotor current by roughly 5.3% and 4.8%, respectively, in the conventional system. The THD in speed, torque, and stator current with P CURRENT CONTROL and P TORQUE CONTROL is decreased by approximately 19% and 36%, respectively, when compared to the article [10] indicate that the suggested P CURRENT CONTROL and P TORQUE CONTROL system with a 2-level converter is better than the standard one. The SRM method provides 10% to 30% more power than an induction motor and doesn't require a modulator, making it the most practical direct control method, along with the P TORQUE CONTROL and P CURRENT CONTROL methods [3]. With the same current, an induction motor can only generate between 70 and 90 per cent of the force generated by an SRM due to its delayed power factor. In this paper, total harmonic distortion (THD) has been accurately computed using MATLAB 2013 in comparison to (10). In contrast to the P CURRENT CONTROL and P TORQUE CONTROL method with a 15-level H-bridge multilevel inverter using an induction motor, which is detailed in the Table.3 [21], the SRM method with a 15-level H-bridge multilevel inverter lowers 23% more THD in power, speed, and stator current. The graphs 1, 2, and 3 also illustrate the graphical representation of the percentage of THD in terms of rotor speed, electromagnetic torque, and stator current. The table also includes comparisons of P CURRENT CONTROL and P TORQUE CONTROL's problems. 4. Switching losses are kept to a minimum because transistors are only turned on when necessary to maintain the limits of torque and flux. To improve the efficiency of a multilevel converter, semiconductor switches are switched in a specific sequence. This plan enhances productivity and reduces costs while minimising switching losses. When compared to P TORQUE CONTROL and P CURRENT CONTROL methods using a 2-level voltage source inverter, Direct Torque Control of Induction Motor (DTC), and Direct Torque Control of Induction Motor with Fuzzy Logic Controller, the 15-level H-bridge multilevel inverter used in this study with SRM and IM provides excellent torque and flux responses, robust, and stable operation is achieved. (DTC with fuzzy). Due to its simple formula and strong results in both stable and transient states, this innovative technique rapidly drew the attention of academics. In terms of speed, torque, and stator current ripple during transient circumstances, the suggested system responds better than the usual one [10]. Fig.5: Current Controller with 15-MLI SRM Result

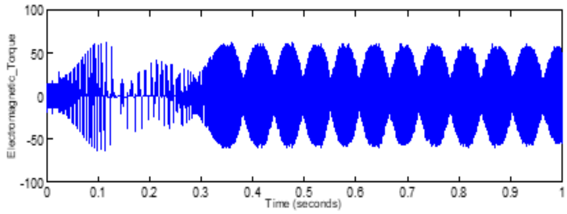

Fig. 5. (a) Electromagnetic Torque in P Current Controller

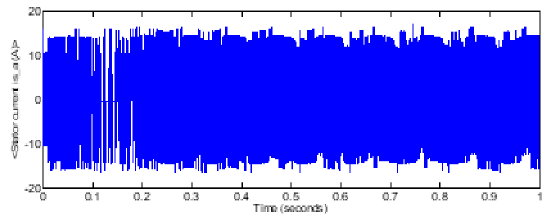

Fig. 5. (b) Stator Current in P Current Controller

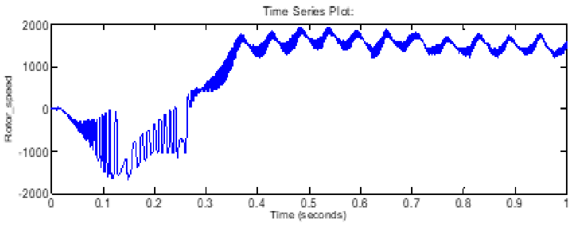

Fig. 5. (c) Rotor speed in P Current Controller

Retrieval Number: 100.1/ijese.E41140612523
DOI: 10.35940/ijese.E4114.12070624
Journal Website: www.ijese.org

Published By:
Blue Eyes Intelligence Engineering and Sciences Publication (BEIESP)

International Journal of Emerging Science and Engineering (IJESE)
ISSN: 2319–6378 (Online), Volume-12 Issue-7, June 2024

Fig.6: PTorque Controller with 15-MLI SRM result

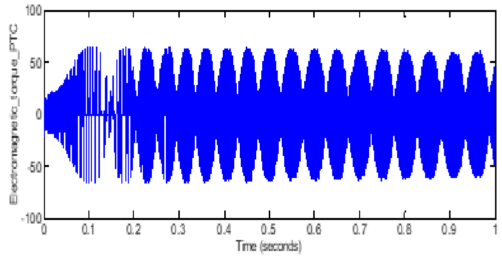

Fig. 6. (a) Electromagnetic Torque in PTorque Controller

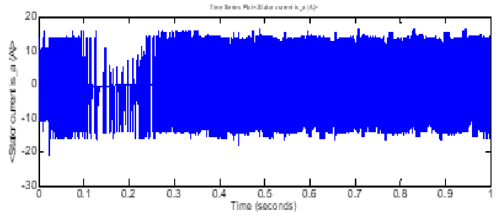

Fig. 6. (b) Stator current in PTorque Controller

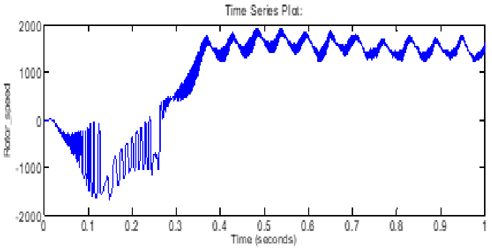

Fig. 6. (c) Rotor speed in PTorque Controller

Fig.7: P P Current Controller with 15-level MLI using IM

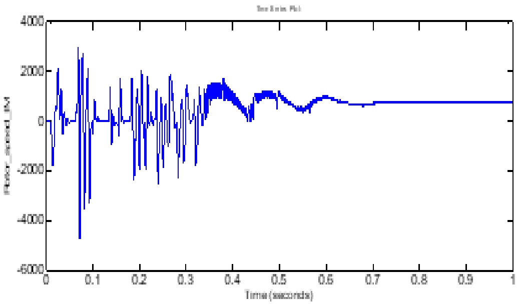

Fig. 7. (a) Speed in P Current Controller

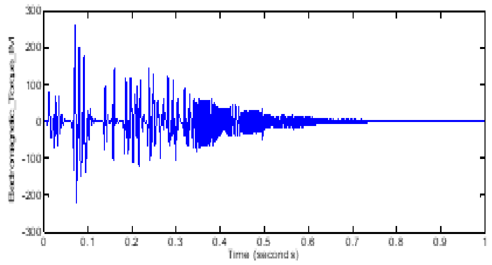

Fig. 7. (b) Torque in P Current Controller

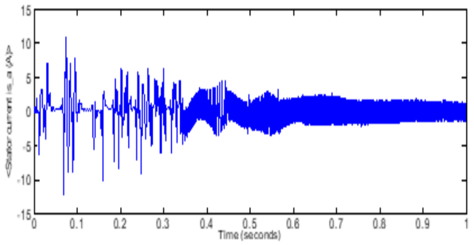

Fig. 7. (c)Current in P Current Controller Stator

Fig.8: P TORQUE CONTROL with 15-level MLI using IM result

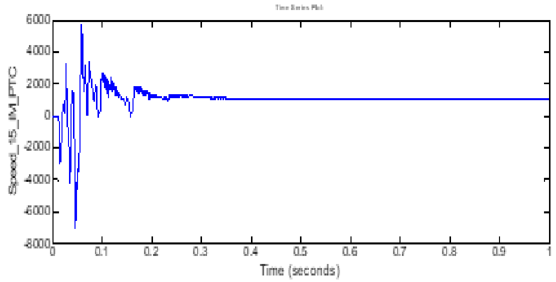

Fig. 8. (a) Speed in PTorque Controller

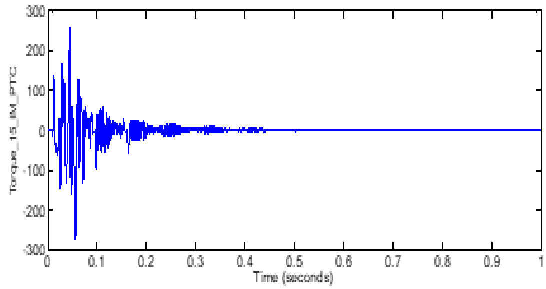

Fig. 8. (b) Torque in PTorque Controller

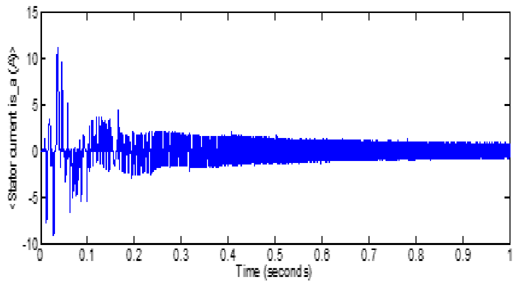

Fig. 8. (c) Current in PTorque Controller

Fig.9: THD in PCurrent Control with 15-level MLI using SRM result

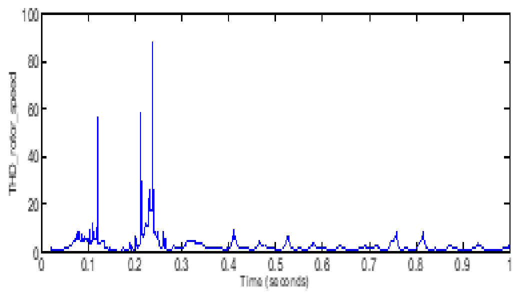

Fig. 9. (a) Rotor Speed Consist THD

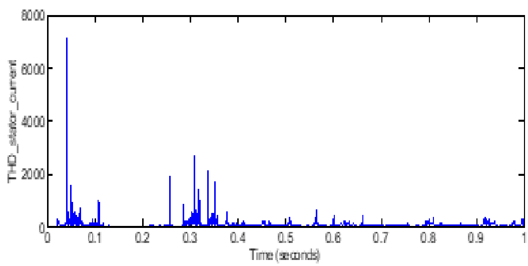

Fig. 9. (b) Stator Current Consists of THD

Retrieval Number: 100.1/ijese.E41140612523
DOI: 10.35940/ijese.E4114.12070624
Journal Website: www.ijese.org

Published By:
Blue Eyes Intelligence Engineering
and Sciences Publication (BEIESP)

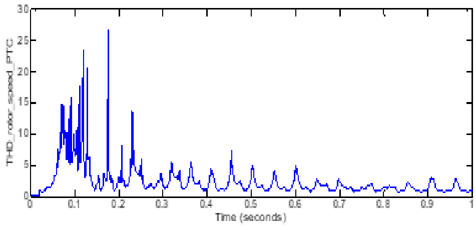

Fig. 9. (c) Torque THD

Fig.10: THD in P TORQUE CONTROL with 15-MLI using usingSRM

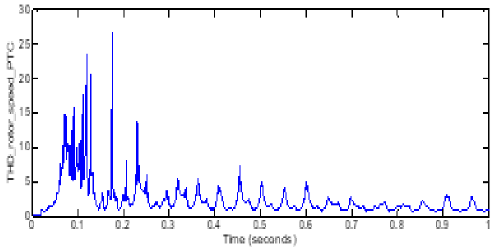

Fig. 10. (a) Rotor Speed THD

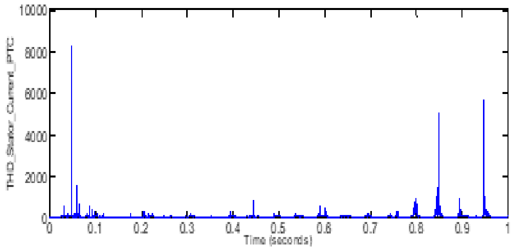

Fig. 10. (b) Stator Current THD

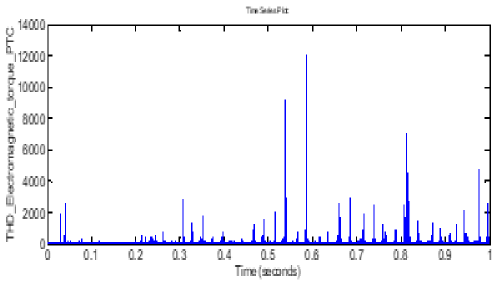

Fig. 10. (c) Torque THD

Fig.11: THD in PCurrent Control with 15-level MLI using IM

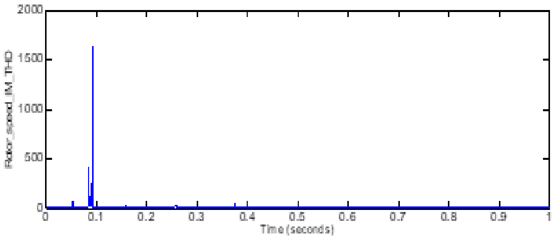

Fig. 11.(a) Rotor Speed THD

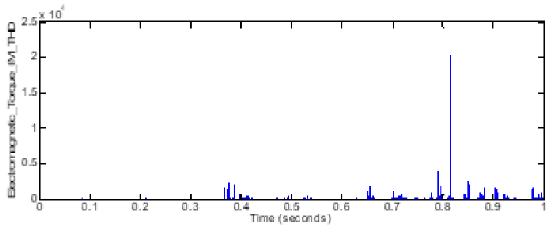

Fig. 11.(b) Torque THD

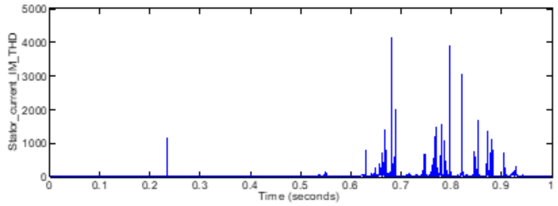

Fig. 11.(c) Stator Current THD

Fig.12: THD in P TORQUE CONTROL with 15-MLI using IM

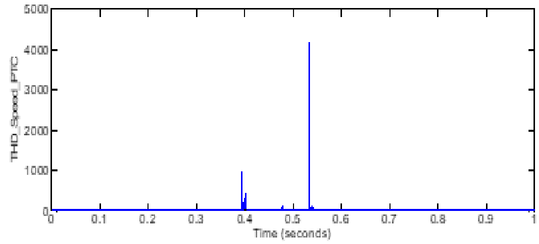

Fig. 12. (a) Rotor Speed THD

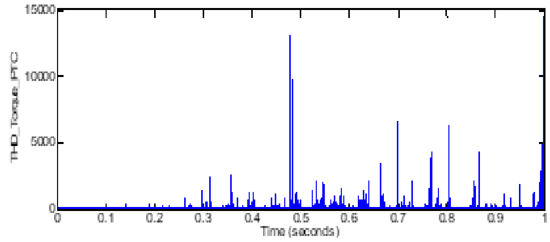

Fig. 12. (b) Torque THD

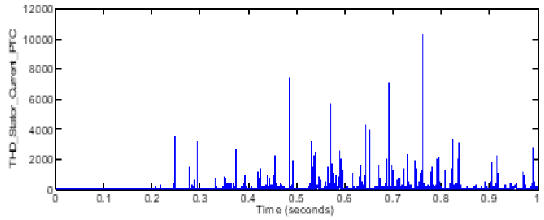

Fig. 12. (c) Stator Current THD

Fig.13: P Current Control with 2-level VSI using SRM

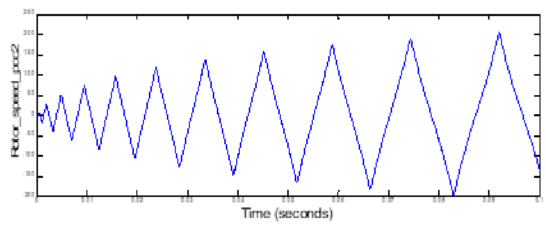

Fig. 13 (a) Rotor speed in P Current Control

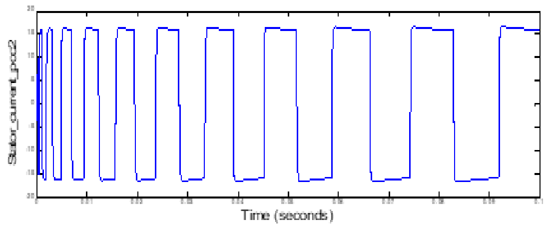

Fig. 13 (b) Stator Current in P Current Control

Retrieval Number: 100.1/ijese.E41140612523
DOI: [10.35940/ijese.E4114.12070624](https://doi.org/10.35940/ijese.E4114.12070624)
Journal Website: www.ijese.org

Published By:
Blue Eyes Intelligence Engineering and Sciences Publication (BEIESP)

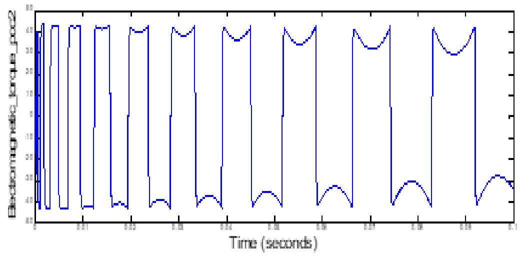

Fig. 13 (c) Obtained Torque in P Current Control

Fig.14: P Torque Control with 2-level VSI using SRM

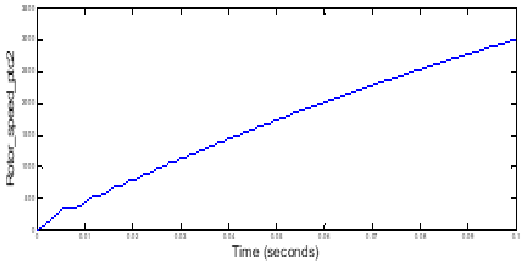

Fig. 14 (a) Rotor Speed in P Torque Control

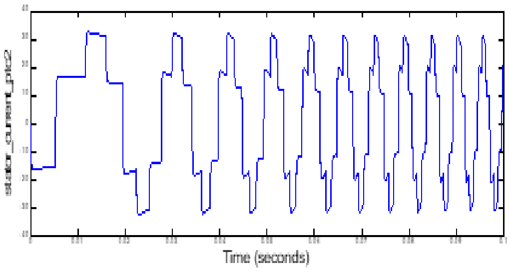

Fig. 14 (b) Stator Current in P Torque Control

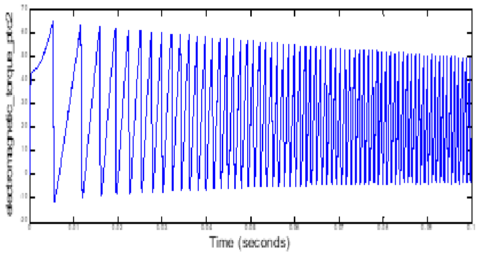

Fig. 14 (c) Obtained Torque in P Torque Control

Fig.15: P Current Control with 2-level VSI using IM

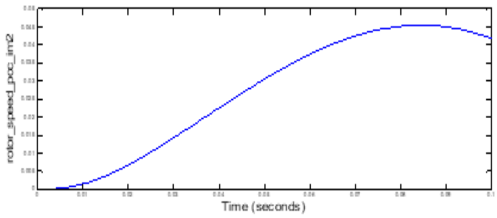

Fig. 15 (a) Rotor Speed in P Current Control

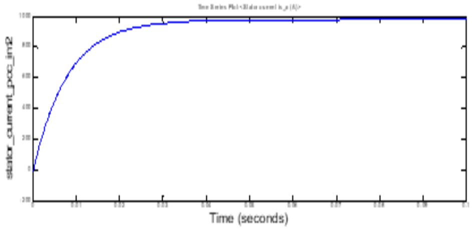

Fig. 15 (b) Stator Current in P Current Control

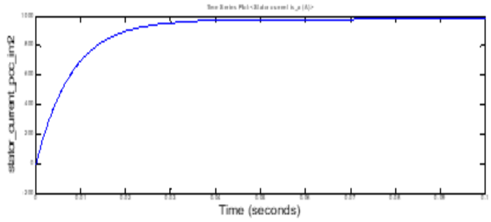

Fig. 15(c) Obtained Torque in P Current Control

Fig.16: P TORQUE CONTROL with 2-level VSI using IM

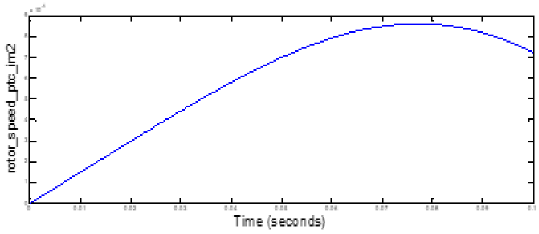

Fig. 16 (a) Rotor Speed in P Torque Control

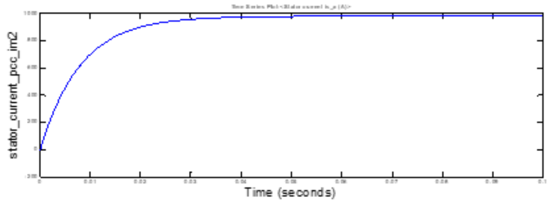

Fig. 16 (b) Stator Current in P Torque Control

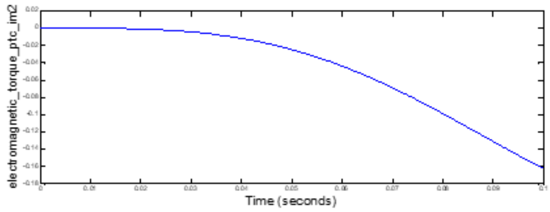

Fig. 16 (c) Obtained Torque in P Torque Control

Fig.17: THD in P CURRENT CONTROL with 2-level VSI using SRM

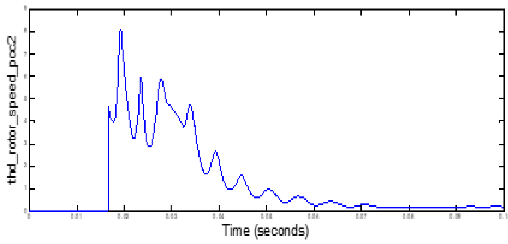

Fig. 17 (a) THD in Rotor Speed

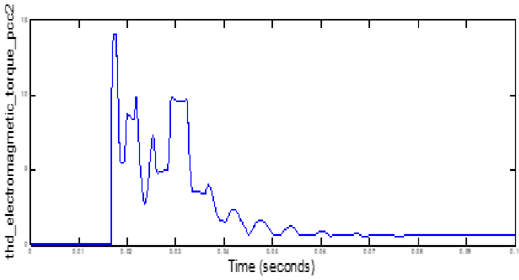

Fig. 17 (b) THD in Electromagnetic Torque

Retrieval Number: 100.1/ijese.E41140612523
DOI: 10.35940/ijese.E4114.12070624
Journal Website: www.ijese.org

Published By:
Blue Eyes Intelligence Engineering and Sciences Publication (BEIESP)

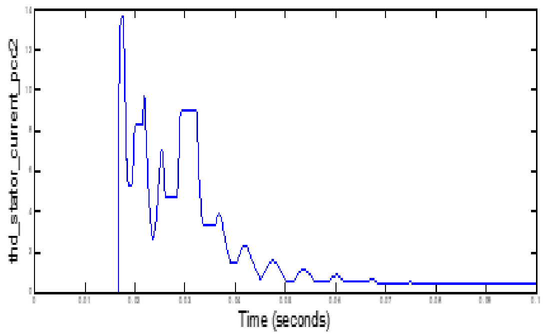

Fig. 17 (c) THD in Stator Current

Fig.18: THD in P Torque Control with 2-level VSI using SRM

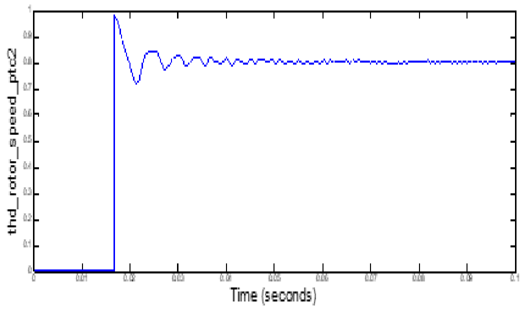

Fig. 18 (a) THD Rotor Speed

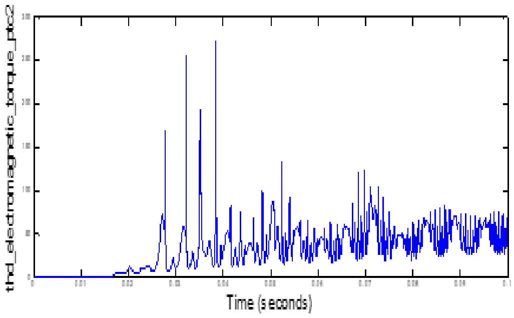

Fig. 18(b) THD Electromagnetictorque

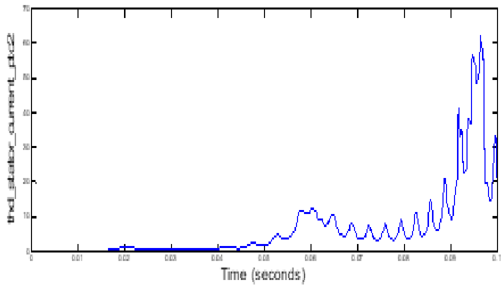

Fig. 18 (c) THD Stator Current

Fig.19: THD in P CURRENT CONTROL with 2-level VSI using IM

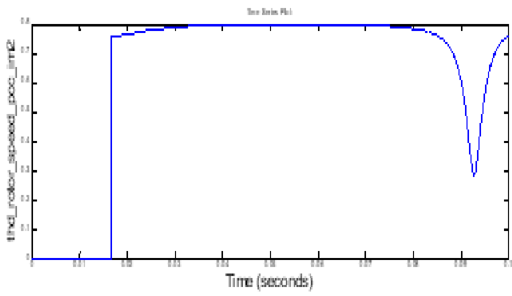

Fig. 19 (a) THD in Rotor Speed

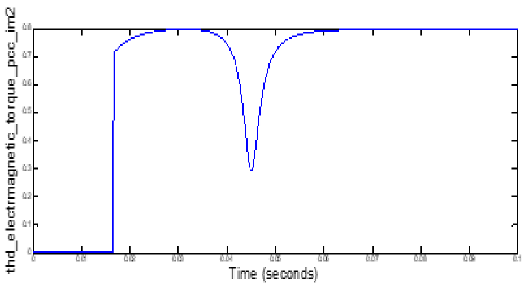

Fig. 19 (b) THD in Electromagnetic Torque

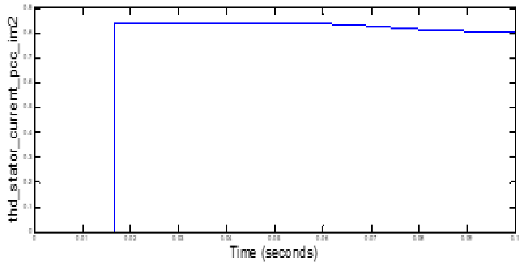

Fig. 19 (c) THD in Stator Current

Fig.20: THD in P Torque Control with 2-level VSI using IM

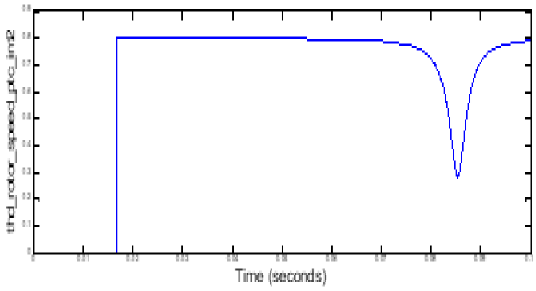

Fig. 20 (a) THD Rotor Speed

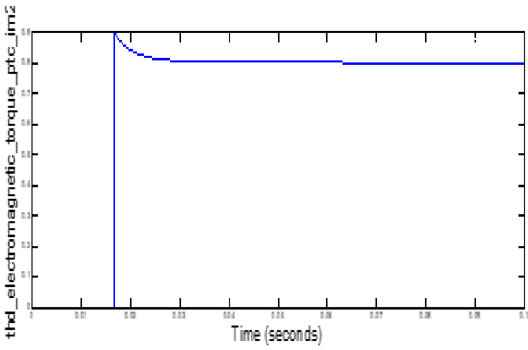

Fig. 20 (b) THD Electromagnetic Torque

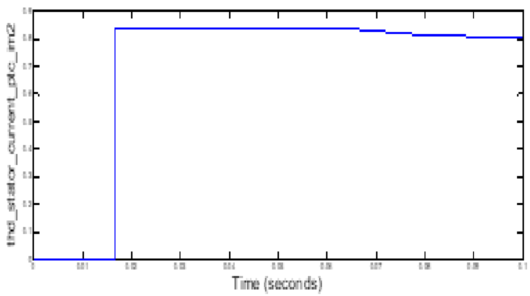

Fig. 20 (c) THD Stator Current

Retrieval Number: 100.1/ijese.E41140612523
DOI: 10.35940/ijese.E4114.12070624
Journal Website: www.ijese.org

Published By:
Blue Eyes Intelligence Engineering
and Sciences Publication (BEIESP)

C. THD Analysis of P Current Control and P Torque Control Method

Table 3: %THD Calculation Comparison

Sr. No	Different Methods	%THD in		
		Rotor Speed (w_r)	Torque (T_e)	Stator Current
1	P CURRENT CONTROL with SRM using 15-level multilevel inverter	31.44	31.34	44.85
2	P TORQUE CONTROL with SRM using 15-level multilevel inverter	21	21	118
3	P CURRENT CONTROL with IM using 15-level multilevel inverter	54.24	155.2	53.22
4	P TORQUE CONTROL with IM using 15-level multilevel inverter	41.51	41.51	89.67
5	P CURRENT CONTROL with SRM using 2-level voltage source inverter(VSI)	82.45	68.60	39.39
6	P TORQUE CONTROL with SRM using 2-level voltage source inverter(VSI)	106.11	41.40	90.02
7	P CURRENT CONTROL with IM using 2-level voltage source inverter(VSI)	118.86	98.14	72.21
8	P TORQUE CONTROL with IM using a 2-level voltage source inverter(VSI)	57.20	79.38	102.34
9	Direct Torque control of IM using 2-level voltage source inverter(VSI)	49.53	81.62	157.84
10	Direct Torque control of IM with Fuzzy Logic Controller using 2-level voltage source inverter(VSI)	49.53	61.82	137.14

D. Comparative Issues between P CURRENT CONTROL and P TORQUE CONTROL

Table 4: Comparative Issues between P Current Control and P Torque Control

Feature	P Current Control	P Torque Control
Conceptual Complexity	Poor	Poor
PI-current controller	Not Req	Not Req
Use of PWM	Not Req	Not Req
Switching Frequency	Varying	Varying
Dynamics	Quick	Quick
Torque Ripple	Higher	Lower
Stator current THD	Poor	Poor
System Constraints Inclusion	Easyly	Easyly

E. Graphical Representation of % THD in Speed, Torque and Stator Current

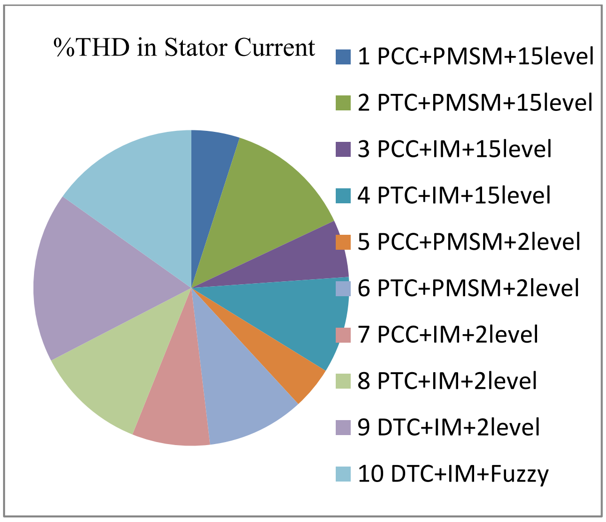

a. Graph-1 THD in Stator

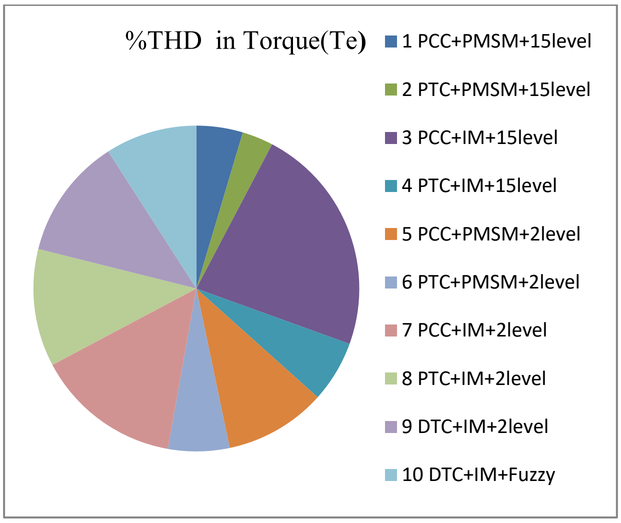

b. Graph-1 THD in Torque

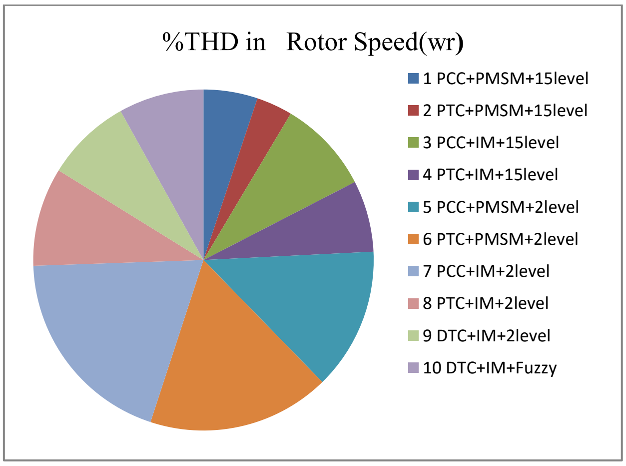

c. Graph-1 THD in Rotor Speed

VIII. CONCLUSION

This paper presents and investigates the P CURRENT CONTROL and P TORQUE CONTROL methods of the MPC family with a 15-level multilevel inverter using solely simulation methodology.

Retrieval Number: 100.1/ijese.E41140612523
DOI: 10.35940/ijese.E4114.12070624
Journal Website: www.ijese.org

Published By:
Blue Eyes Intelligence Engineering and Sciences Publication (BEIESP)

Compared to the P TORQUE CONTROL method with a 15-level multilevel inverter, the P CURRENT CONTROL method has a quicker computation time, a quicker dynamic reaction, and reduced stator current harmonics. Without an interior current PI controller or a modulator, both techniques are direct control techniques.

The P CURRENT CONTROL technique is more effective for uses with extended prediction horizons as a result of this benefit. According to the test findings, the P CURRENT CONTROL method and the P TORQUE CONTROL method with a 15-level multilevel inverter both work admirably in constant and transient conditions. The P CURRENT CONTROL method with a 15-level multilevel inverter is superior when the currents are assessed. Still, the P TORQUE CONTROL method with a 15-level multilayer inverter has fewer torque ripples. Due to its simple formula and strong results in both stable and transient states, this innovative technique rapidly drew the attention of academics.

Future research will evaluate switched reluctance motors, and when P CURRENT CONTROL and P TORQUE CONTROL methods are applied to servo motors with multiple inverters, we expect that the computation time will be significantly reduced. The P TORQUE CONTROL method exhibits significantly greater resilience to the magnetising inductance than the P CURRENT CONTROL method does to the stator resistance.

DECLARATION STATEMENT

Funding	No, I did not receive.
Conflicts of Interest	No conflicts of interest to the best of our knowledge.
Ethical Approval and Consent to Participate	No, the article does not require ethical approval or consent to participate, as it is based on evidence.
Availability of Data and Materials	Not relevant.
Authors Contributions	All authors have equal participation in this article.

REFERENCES

1. Patricio Cortés, Marian P. Kazmierkowski, and Ralph M. Kennel, Daniel E. Quevedo, and José Rodríguez, "Predictive Control in Power Electronics and Drives," IEEE Transactions On Industrial Electronics, VOL. 55, NO. 12, Dec. 2008 https://doi.org/10.1109/TIE.2008.2007480
2. Georgios Papafotiou, Jonas Kley, Kostas G. Papadopoulos, Patrick Bohren, and Manfred Morari, "Model Predictive Direct Torque Control—Part I: Implementation and Experimental Evaluation," IEEE Transactions On Industrial Electronics, VOL. 56, NO. 6, JUNE 2009 https://doi.org/10.1109/TIE.2008.2007032
3. Georgios Papafotiou, Jonas Kley, Kostas G. Papadopoulos, Patrick Bohren, and Manfred Morari, "Model Predictive Direct Torque Control—Part II: Implementation and Experimental Evaluation," IEEE Transactions On Industrial Electronics, VOL. 56, NO. 6, JUNE 2009 https://doi.org/10.1109/TIE.2008.2007032
4. Thomas Burtscher and Tobias Geyer, "Deadlock Avoidance in Model Predictive Direct Torque Control," IEEE Transactions On Industry Applications, Vol. 49, No. 5, September/October 2013. https://doi.org/10.1109/TIA.2013.2261445
5. Tobias Geyer, "Model Predictive Direct Torque Control: Derivation and Analysis of the State-Feedback Control Law," IEEE Transactions on Industry Applications, Vol. 49, No. 5, September/October 2013 https://doi.org/10.1109/TIA.2013.2262255
6. James Scoltock, Tobias Geyer and Udaya K. Madawala, "A Comparison of Model Predictive Control Schemes for MV Induction Motor Drives," IEEE Transactions on Industrial Informatics, Vol. 9, No. 2, May 2013 https://doi.org/10.1109/TII.2012.2223706
7. Yongchang Zhang and Haitao Yang, "Model Predictive Controller of Torque of Induction Motor Drives With Optimal Duty Cycle Control," IEEE Transactions on Power Electronics, Vol. 29, No. 12, December 2014 https://doi.org/10.1109/TPEL.2014.2302838
8. Fengxiang Wang, Zhenbin Zhang, S. AlirezaDavari, Reza Fotouhi, Davood Arab Khaburi, José Rodríguez, and Ralph Kennel, "An EncoderlessPredictive controller of torque for an Induction Machine With a Revised Prediction Model and EFOSMO," IEEE Transactions On Industrial Electronics, Vol. 61, No. 12, December 2014 https://doi.org/10.1109/TIE.2014.2317140
9. Petros Karamanakos, Peter Stolze, *Student Member,* Ralph M. Kennel, Stefanos Manias, and Hendrik du Toit Mouton, "Variable Switching Point Predictive controller of torque of Induction Machines," IEEE Journal of Emerging and Selected Topics in Power Electronics, Vol. 2, No. 2, June 2014 https://doi.org/10.1109/JESTPE.2013.2296794
10. Fengxiang Wang, *Member, IEEE*, Shihua Li, *Senior Member, IEEE*, Xuezhu Mei, Wei Xie, *Member, IEEE*, José Rodríguez, *Fellow, IEEE*, and Ralph M. Kennel, *Senior Member, IEEE*, "Model-Based Predictive Direct Control Strategies for Electrical Drives: An Experimental Evaluation of P TORQUE CONTROL and P CURRENT CONTROL Methods," IEEE Transactions On Industrial Informatics, Vol. 11, No. 3, June 2015 https://doi.org/10.1109/TII.2015.2423154
11. Md. Habibullah, *Student Member, IEEE,* and Dylan Dah-Chuan Lu, *Senior Member, IEEE*, "A Speed-Sensorless FS-P TORQUE CONTROL of Induction Motors Using Extended Kalman Filters," IEEE Transactions On Industrial Electronics, Vol. 11, No. 3, Aug 2015 https://doi.org/10.1109/TIE.2015.2442525
12. Takahashi and T. Noguchi, "A new quick-response and high-efficiency control strategy of an induction motor," IEEE Trans. Ind.. Appl., vol. 22, no. 5, pp. 820–827, Sep. 1986. https://doi.org/10.1109/TIA.1986.4504799
13. I. Takahashi and Y. Ohmori, "High-performance direct torque control of an induction motor," IEEE Trans. Ind.. Appl., vol. 25, no. 2, pp. 257–264, Mar./Apr. 1989. https://doi.org/10.1109/28.25540
14. M. Morari and J. Lee, "Model predictive control: Past, present and future," Comput. Chem. Eng., vol. 23, no. 4, pp. 667–682, 1999. https://doi.org/10.1016/S0098-1354(98)00301-9
15. J. Holtz and S. Stadtfeldt, "A predictive controller for the stator current vector of AC machines fed from a switched voltage source," in Proc. IEEE Int. Power Electron. Conf. (IPEC), Mar. 27–31, 1983, vol. 2, pp. 1665–1675.
16. R. Kennel and D. Schöder, "A predictive control strategy for converters," in Proc. IFAC Control Power Electron. Elect. Drives, 1983, pp. 415–422. https://doi.org/10.1016/B978-0-08-030536-3.50061-1
17. M. Preindl and S. Bolognani, "Model predictive direct torque control with finite control set for SRM drive systems, part 1: Maximum torque per ampere operation," IEEE Trans. Ind. Informat., vol. 9, no. 4, pp. 1912–1921, Nov. 2013. https://doi.org/10.1109/TII.2012.2227265
18. M. Preindl and S. Bolognani, "Model predictive direct torque control with finite control set for SRM drive systems, part 2: Field weakening operation," IEEE Trans. Ind. Informat., vol. 9, no. 2, pp. 648–657, May 2013. https://doi.org/10.1109/TII.2012.2220353
19. C. Rojas et al., "Predictive torque and flux control without weighting factors," IEEE Trans. Ind. Electron., vol. 60, no. 2, pp. 681–690, Feb. 2013. https://doi.org/10.1109/TIE.2012.2206344
20. J. Rodriguez *et al.*, "State of the art of finite control set model predictive control in power electronics," *IEEE Trans. Ind. Informat.*, vol. 9, no. 2, pp. 1003–1016, May 2013. [17] J. Rodriguez *et al.*, "Predictive controller of current of a voltage source inverter," *IEEE Trans. Ind. Electron.*, vol. 54, no. 1, pp. 495–503, Feb. 2007. https://doi.org/10.1109/TIE.2006.888802
21. SurajKarpe, Sanjay.A.Deokar, Arati M.Dixit,""Switching losses minimization and performance improvement of P CURRENT CONTROL and P TORQUE CONTROL methods of model predictive direct torque control drives with 15-level inverter", JESIT, vol.1 December 2017. https://doi.org/10.1016/j.jesit.2017.01.009
22. SurajKarpe, Sanjay.A.Deokar, Ulhas B. Shinde, "Improved Performance of Direct Torque Control with PMSM compared to DTC with Induction Motor", TURCOMAT, vol.1, December 2017.

Retrieval Number: 100.1/ijese.E41140612523
DOI: 10.35940/ijese.E4114.12070624
Journal Website: www.ijese.org

Published By:
Blue Eyes Intelligence Engineering and Sciences Publication (BEIESP)

AUTHORS PROFILE

Suraj R. Karpe, Ph.D. in Electrical Machines and Drives from SPPU Pune, in 2019. The interest of the research topic is Switching Losses Minimization and performance improvement of Induction Motor

Sanjay Deokar, Ph.D. in Power quality of Electrical disturbances from Nanded, Dr.Babasaheb Ambedkar Marathwada University in 2016. The interest of the research topic is the Mitigation of all power quality disturbances in the power system

Dr. Ulhas B. Shinde, working as a Principal since 2013 at CSMSS, Chh. Shahu College of Engineering, Aurangabad. Planning and Execution of Academic and Non-Academic Activities. The institute has an overall administration with a student strength exceeding 2,000 and a staff strength of 150. Providing Guidance and Mentoring to HODs, Staff and Students of all Departments. Monitoring and guiding members in preparing proposals and documents related to AICTE, DTE, Universities, Shikshan Shulka Samiti, and Admission-Regulating Authorities. Continuous monitoring of the activities of the NBA, NAAC, and NIRF is carried out by the departments. Established Strong Institute Industry Relations and associated with organizations like CMIA, MASIA, BOAT, CII etc.

Retrieval Number: 100.1/ijese.E41140612523
DOI: [10.35940/ijese.E4114.12070624](https://doi.org/10.35940/ijese.E4114.12070624)
Journal Website: www.ijese.org

Published By:
Blue Eyes Intelligence Engineering
and Sciences Publication (BEIESP)